



# Influence of nonwoven interleave layer on interlaminar fracture of sandwich-structured composites

Zain Ali<sup>1)</sup>, Jakob Schmidt<sup>1)</sup>, Jörg Kaufmann<sup>1)</sup>, Holger Cebulla<sup>1)</sup>

<sup>1)</sup> Department of Textile Technologies, zain.ali@s2018.tu-chemnitz.de, jakob.schmidt@mb.tu-chemnitz.de, joerg.kaufmann@mb.tu-chemnitz.de, holger.cebulla@mb.tu-chemnitz.de, Chemnitz University of Technology, Reichenhainer Straße 70, 09126 Chemnitz, Germany

## Keywords

Cohesive Zone Modelling, Flexural Testing, Nonwoven Interleave Layer, Sandwich-Structured Composite, Skin-Core Debonding

## Abstract

Debonding between the skins and the core is one of the critical failure modes encountered by sandwich-structured composites in highly strained conditions. The onset and growth of a debond critically hinder the load-bearing capacity of the sandwich structure. This paper investigates the effect on the debonding resistance of a sandwich-structured composite by the addition of nonwoven flax interleave veil in the skin-core interface. Mode-II fracture toughness is estimated through a proposed method based on curve fitting of numerical data to experimental results. Experimental data are obtained in a four-point bending test following the standard DIN 53 293 and Cohesive Zone Modelling (CZM) is implemented as the numerical tool in the analysis of Mode-II skin-core debonding. A series of sandwich specimens are fabricated using twill weave e-glass fabric and expanded polystyrene core with and without the addition of an interleave layer. Numerical data show a 60 % increment in Mode-II fracture toughness with the inclusion of a flax interleaf layer. Microscopic images attribute the increment to the presence of fibre bridging effect. The proposed method produces a good fit of numerical data to experimental results.

## 1 Introduction

Sandwich-structured composites are actively being used in various industries for the manufacturing of goods ranging from recreational sports equipment to aircraft components [1]. The combination of thin and stiff face-skins along with a thick and low-density core gives them the advantage of having excellent flexural stiffness to weight ratio. However, sandwich structures under operational load exhibit various failure modes. One of the biggest challenges faced under impact and fatigue load is the propensity of these structures to fracture via skin-core debonding. Debonding leads to a drastic reduction of the structure's stiffness, aiding in the occurrence of further structural failures such as skin buckling under compression [2]. Past research on composite laminates has shown a modest increment in both Mode-I and Mode-II fracture toughness with the addition of a nonwoven polyester and various other synthetic-based interleaf veils in the interface zone [3–5].

Further challenges are encountered in the experimental determination of fracture mechanic properties ( $G_{Ic}$  and  $G_{IIc}$ ) of sandwich-structured composites as no testing standards and data-reduction techniques as of date are available. Researchers have adopted standards for interlaminar fracture toughness of unidirectional fiber-reinforced polymer matrix composites such as ASTM D5528, WK22949, D6671 to sandwich structures [6–8].

This paper explores the possibility of improving the fracture toughness of a woven glass fabric-based sandwich structure by the incorporation of a nonwoven flax veil in the interface region, i.e., in-between the skin-core interface. This paper additionally investigates and implements an approach proposed by Barbero and Shahbazi (2017), which is based on curve fitting of numerical data to experimental data by using Design of Experiments (DoE) and Response Surface Optimization (RSO) in ANSYS workbench, in conjunction with Cohesive Zone Modelling (CZM) to estimate the Mode-II fracture toughness ( $G_{IIc}$ ) of the investigated sandwich specimens in a four-point bending test [9].

Digital Object Identifier: <http://dx.doi.org/10.21935/tls.v5i1.153>  
[www.lightweight-structures.de](http://www.lightweight-structures.de)

This is an open access article under the CC BY 4.0 license (<http://creativecommons.org/licenses/by/4.0/>)

## 2 Materials and methods

### 2.1 Test specimens

Four sandwich-structured composite specimens were fabricated, each having a different face-skin configuration but an identical foam core. Two of the samples were fabricated without the addition of an interleaf layer, to be used as benchmarks for performance comparison. An overview of the layup configuration of each specimen is given in Table 1.

Table 1: Overview of the specimens skin configuration

	Specimen I	Specimen II	Specimen III	Specimen IV
Top Skin Layer I	E-Glass	E-Glass	E-Glass	E-Glass
Top Skin Layer II	-	E-Glass	-	E-Glass
Interface Layer	-	-	Spunlaced Flax	Spunlaced Flax
Core	XPS300	XPS300	XPS300	XPS300
Interface Layer	-	-	Spunlaced Flax	Spunlaced Flax
Bottom Skin Layer II	-	E-Glass	-	E-Glass
Bottom Skin Layer I	E-Glass	E-Glass	E-Glass	E-Glass

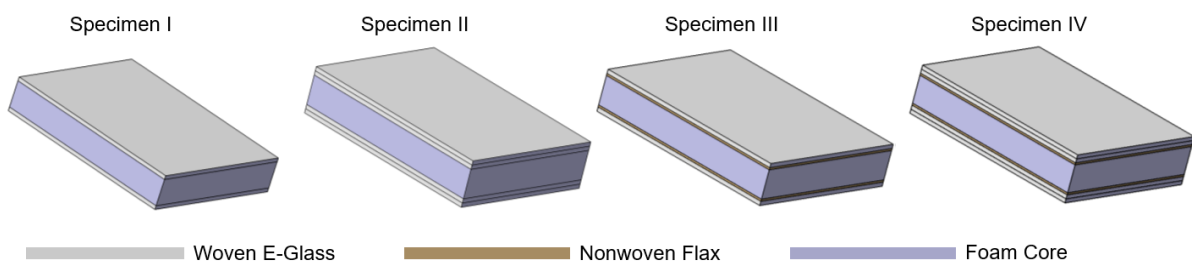


Figure 1: Schematic of the specimens

Face-skins of specimens I & II were fabricated using one and two layers of twill weave e-glass fabric reinforced plastic, respectively, which is orthotropic in nature with a fiber content of 39 % and a young's modulus of 25.4 GPa [10]. The commercially available woven e-glass fabric was supplied by R&G Faserverbundwerkstoffe GmbH. XPS 300, made of extruded polystyrene, was used as the foam core for each of the sandwich specimens. XPS 300 foam is isotropic in nature and has a closed-cell structure. The face-skins of specimens III & IV were fabricated using one and two layers, respectively, of the same twill weave e-glass fabric with the addition of a single nonwoven flax interleaf in the skin-core interface. The high absorbent spunlaced flax veil supplied by Norafin industries yielded a fiber volume content of 24 % and a young's modulus of 6.1 GPa, obtained from the performed test following DIN EN ISO 527-4 standard. Super Sap 305 epoxy resin supplied by Entropy Resins in combination with CPS slow hardener was used in the fabrication of the specimens. Mechanical properties of the individual materials are summarized in Table 2.

Table 2: Material data

Characteristic	Woven e-glass fabric	Nonwoven flax veil	XPS 300 foam
Areal weight	163 g/m <sup>2</sup>	80 g/m <sup>2</sup>	-
Fabric Thickness	0.20 mm	0.55 mm	20 mm
Ply thickness	0.24 mm	0.31 mm	20 mm
φF	37 %	24 %	-
E11 = E22 / E33	17 / 3.40 GPa	6.1 / 3.4 GPa	15.0 MPa
ν12 / ν13 = ν23	0.10 / 0.30	0.11 / 0.37	0.36
G12 = G13 = G23	4.20 GPa	1.5 GPa	5.47 MPa

The sandwich components were manufactured in a wet hand lay-up process and vacuum bagged for twenty-four hours at room temperature for consolidation. The samples were afterwards post-cured in an oven at 60°C for sixty minutes, to ensure complete crosslinking in the reactive resins. Eight test coupons from each consolidated sandwich panel were machined using a power-saw and sized in accordance with the DIN 53 293 standard.

## 2.2 Four-point bending test

In a previous study involving similar sandwich-structured composites in a long-span flexural test, it was observed that the primary failure mode of the test coupons was tangential skin-core debonding at the interface under compression. Therefore, this paper investigates the possibility of extracting the Mode-II fracture toughness ( $G_{IIc}$ ) of the test coupons in a four-point bending test setup. The bending load-deformation behavior of the sandwich test coupons was investigated following the DIN 53 293 standard. Tests were performed in a universal testing machine (Zwick/Roell Z010) fitted with a four-point flexural bending attachment at a loading rate of 10 mm/min. Loading and supporting pins used were 30 mm wide to prevent local indentation failure. Inner and outer span were fixed at 200 mm and 400 mm, respectively. Eight samples of each specimen were tested to failure. The applied load ( $F$ ) and displacement ( $\delta$ ) in the four-point bending tests were recorded using a data logger.

## 2.3 Numerical analysis methodology

### 2.3.1 Cohesive Zone Modelling (CZM)

CZM combines the concept of damage mechanics and fracture mechanics to predict both debond initiation and propagation. Fracture is regarded as a gradual phenomenon in which separation takes place across an extended crack tip in the interface. CZM simulates the behaviour of an interface by defining a softening law that relates cohesive traction ( $\sigma$ ) to the corresponding interfacial separation ( $u$ ) between the interacting surfaces. In the conducted numerical analysis contact elements and bilinear softening law was used. Mode-II critical fracture energy is computed using the formulation:

$$G_{IIc} = \frac{1}{2} \tau_0 u_c^t \quad (1)$$

The maximum tangential contact stress is referred to as  $\tau_0$ , whereas the tangential slip at the completion of debonding is defined as  $u_c^t$ .

### 2.3.2 Numerical model

The numerical model was designed in the finite element software ANSYS, depicting exact geometrical dimensions of the fabricated test samples, and maintaining testing conditions as specified in the standard DIN 53 293. Given the geometrical symmetry one-fourth of the model was simulated as shown in Figure 2 a). Contact elements with a bilinear material model were used to represent the cohesive zone in the skin-core interface. The critical Mode-II fracture energy ( $G_{IIC}$ ) of each specimen was found through curve fitting of numerical results, using Design of Experiments (DoE) and Response Surface Optimization (RSO), to experimental data obtained from a four-point bending test.

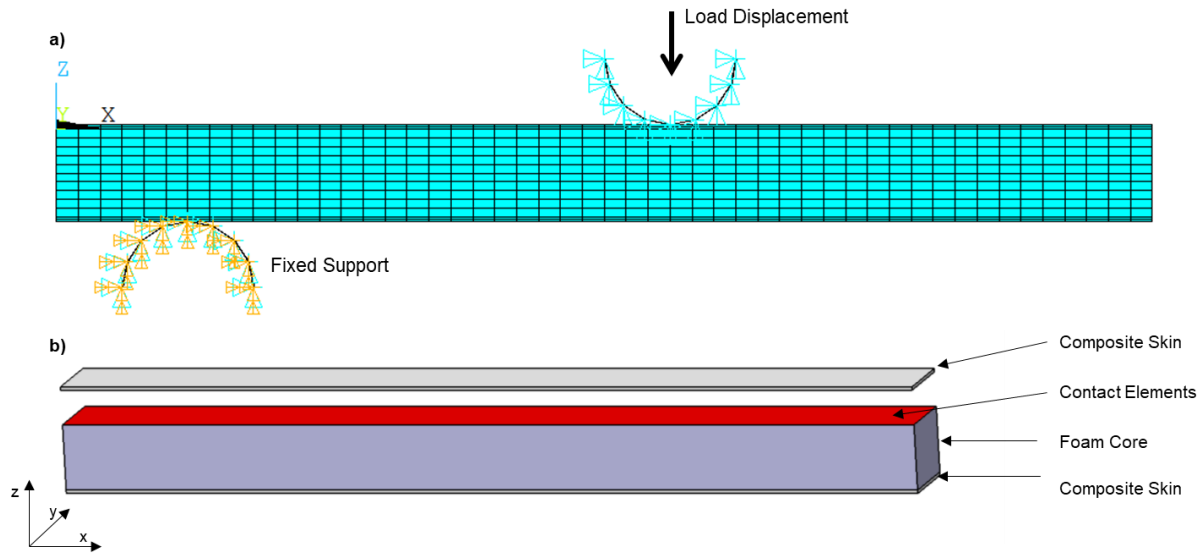


Figure 2: Finite Element Model: a) boundary conditions, b) schematic of the model

### 2.3.3 Curve fitting

Considering the non-linear nature of this FEM analysis, direct evaluation of numerous sampling points of  $G_{IIC}$  for curve fitting would be computationally expensive. An alternative to this is to use a multivariate quadratic polynomial, known as Response Surface (RS), to approximate an output function (E). RS approximates a relationship between the input variables and output function and finds ideal operating conditions for the given process or for a region of the factor field that satisfies the user-defined operating constraints. RS can be constructed with just a few direct evaluations of the finite element model using a handful of sampling points, that are carefully chosen by DoE as the input parameters. DoE locates sampling points within a user-defined design space in a way that the resultant statistical model has low uncertainty in its model estimation and thus high prediction accuracy. The output function (E) here is defined as the difference (error) between numerical results and experimental data (four-point bending test):

$$E = \frac{1}{N} \sqrt{\sum_{i=1}^N [F(u)^{ansys} - F(u)^{exp.}]^2} \quad (2)$$

$F(u)$  is the applied force as a function of load-point deflection, and  $N$  is the number of experimental data points available from the four-point bending test. This user-defined output function (E) was scripted using ANSYS Parametric Design Language (APDL) and imported directly into the post-processor of ANSYS Mechanical. The script computes the error (E) by performing finite element analysis for a given set of input CZM material parameters ( $G_{IIC}, \tau_0$ ) as selected by the DoE within the user-specified range. The CZM material properties are then found by minimizing the output function (E) by using Response Surface Optimization (RSO), which statistically predicts material properties ( $G_{IIC}, \tau_0$ ) that result in the closest fitting curve to the experimental data.

### 3 Results

#### 3.1 Experimental results

The load-displacement data set of the tested coupons for each specimen were averaged and the resulting mean curves are shown in Figure 3.

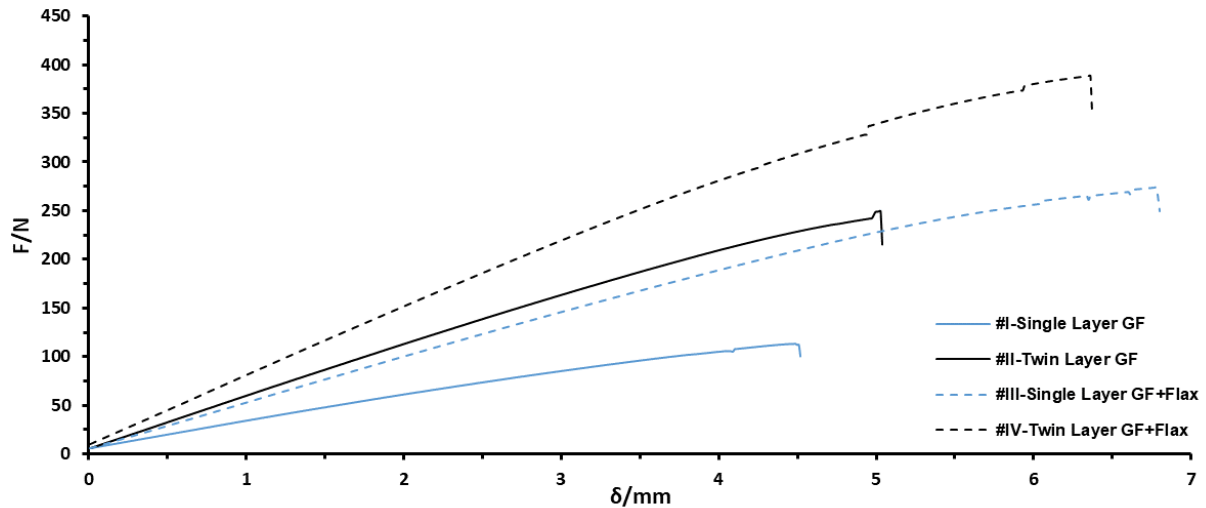


Figure 3: Load-displacement curves from the four-point bending test

The load-displacement curves begin with an increasing linear function followed by a slight decline. At reaching peak loads failure was governed by the weak interfacial strength as each specimen exhibited a similar failure mode, i.e., debonding of the skin-core interface as illustrated in Figure 4. No visible indentation failure or shear cracking of the core was observed.

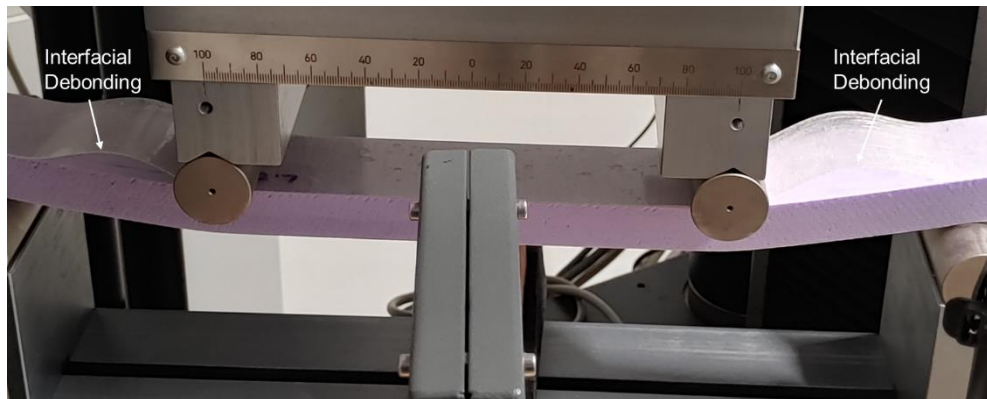


Figure 4: Test specimen #II in a four-point bending test

Sandwich specimens with the addition of a nonwoven flax interleaf layer have shown significant improvement in flexural strength in comparison to their counterparts. Specimen #III and #IV failed at higher peak loads, which is expected due to the stiffening effect of the additional layer. On the contrary, this could also be attributed to the increase in fracture toughness of the specimen, as the midspan deflection length at which failure was observed increased by 35 % on average. Comparing curves of specimen #II and #III, although both have a two-layered skin configuration, specimen #III with the flax layer has exhibited a 7 % improved flexural strength. Albeit the woven glass layer has superior mechanical properties than flax (refer to Table 2), the improvement in fracture toughness due to the inclusion of flax has allowed the structure to maintain its structural integrity and therefore its load-bearing capacity.

The fractured samples were placed under a digital microscope to investigate the probable mechanism behind the improved performance. Figure 5 shows microscopic photos of the lateral surface of the debonded region. The presence of bridging fibres can be seen at the crack tip in Figure 5 b) with the addition of the nonwoven flax in comparison to Figure 5 a) without the nonwoven flax. Results are analogous to investigations concluded by Kuwata and Hogg (2011) on nonwoven interleaf veils [5]. In fibre bridging phenomenon, the pulled-out fibres act as crack arrestors by bridging the debonding front through a pinning mechanism creating a stress-shielding effect at the crack tip. This leads to an increase in fracture resistance, requiring additional load to produce a further increment in the crack. A probable cause for the increase in fibre pull-out and bridging could be attributed to the interaction of the propagating crack with the misaligned or inclined fibres of the nonwoven veil [11].

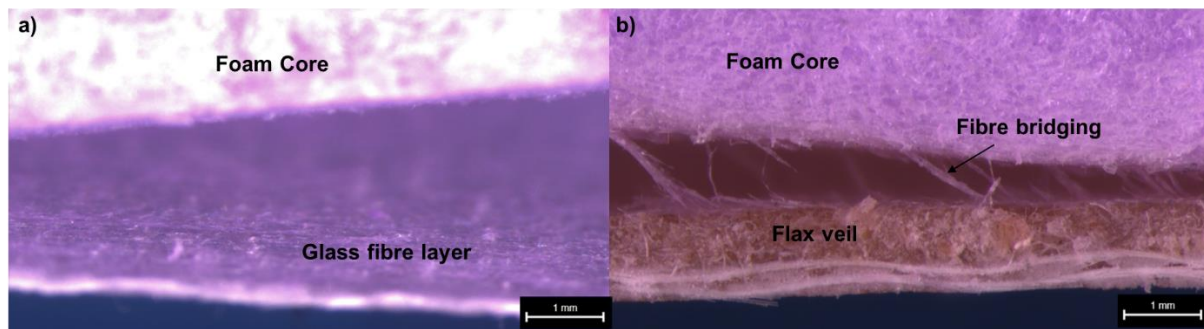


Figure 5: Microscopic photos of the debonded region: a) #II-Twin layer GF, b) #IV-Twin layer GF+Flax

### 3.2 Numerical results

Ten numerical evaluations were required to generate the response surface for each of the four specimens. Estimated CZM parameters are given in Table 3 and their respected load-displacement curves are shown in Figure 7.

Table 3: Estimated fracture mechanic properties

Specimen #	Max. Tangential Contact stress ( $\tau_0$ )	Critical Fracture Energy ( $G_{IIC}$ )
I-Single layer GF	0.047 MPa	0.0405 kJ/m <sup>2</sup>
II-Twin layer GF	0.128 MPa	0.0478 kJ/m <sup>2</sup>
III-Single layer GF + Flax	0.134 MPa	0.0638 kJ/m <sup>2</sup>
VI-Twin layer GF + Flax	0.198 MPa	0.0765 kJ/m <sup>2</sup>

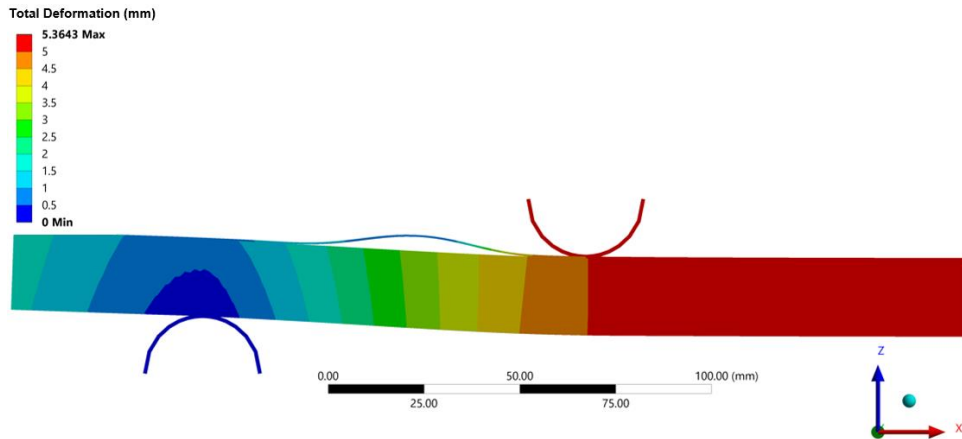


Figure 6: Deformation contour of specimen #II showcasing interfacial debonding as predicted by FEA

Debonding was caught by the numerical model with good approximation as seen in Figure 6. Estimated values show an increment of almost 60 % in the critical fracture energy of the specimens after the addition of flax. Estimated  $G_{IIC}$  values show an increasing trend with increasing ply thickness of the skin. This is conventional behaviour given fracture toughness of sandwich-structured composites is not a material property but rather structural depending on a host of factors, including skin configuration, core material, resin system, and fabrication process.

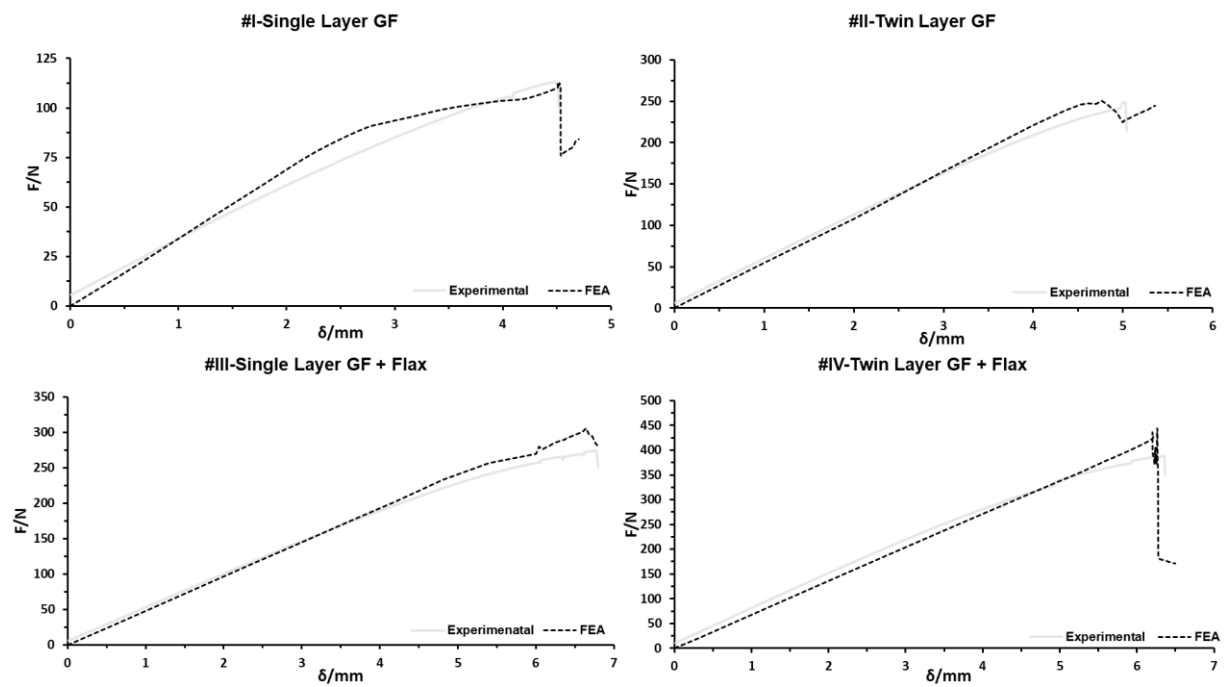


Figure 7: Comparison between numerical and experimental load-displacement curves

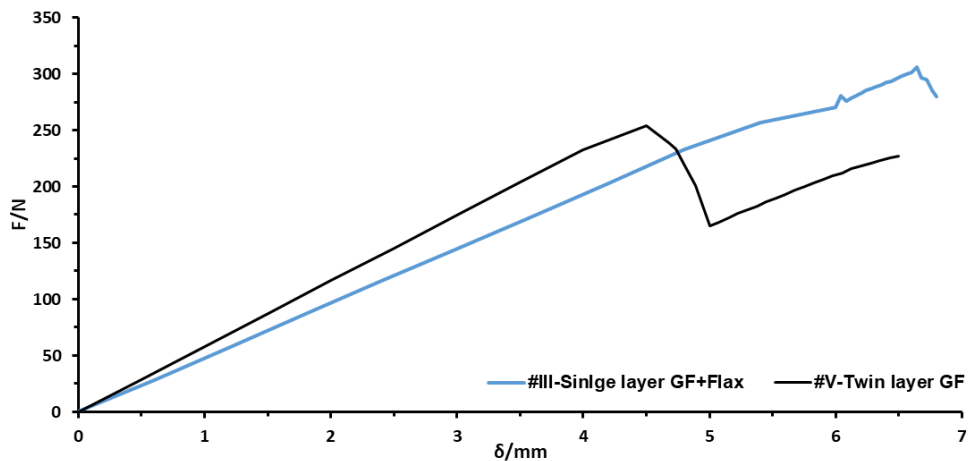


Figure 8: Load-displacement curves of specimen #III and #V

For better comparison and to mitigate the influence of the skin thickness on the flexural strength, two sandwich specimens (#III and #V) with identical skin thicknesses of 0.55 mm were numerically simulated using the obtained fracture mechanic properties (Table 3), #III weighing 13.4 g and #V 15.8 g, respectively. An improvement of 21 % in flexural strength from the specimen with the flax layer can be seen in the curves in Figure 8, signifying the influence of fracture toughness on the overall performance of the structure.

#### 4 Discussion and conclusion

Experimental and numerical behavior of skin-core interface debonding of a sandwich-structured composite has been presented. Four specimens with different skin configurations were considered with the aim of studying the effect of the addition of a nonwoven flax interleaf layer on the fracture toughness. Numerical results have shown an increment of almost 60 % in Mode-II critical fracture energy with the inclusion of the flax layer. This translates to an improvement of 21 % in flexural strength in specimen configured with a nonwoven flax layer against a similar sized specimen without flax. Lastly, the overlapping of the load-displacement curves was kept in good approximation by the proposed numerical method.

It is noteworthy that within RSO, optimization is performed using the response surface rather than an actual evaluation of the response via finite element analysis (FEA). This has the advantage of a significant reduction in computer time; on the contrary, the results are only an approximation to the actual output function (E). Nevertheless, past research has shown response surface to be fairly accurate when compared to direct optimization [9].

The numerical model failed to precisely mimic the non-linear segment of the curves before failure. This could be improved by applying an appropriate failure criterion to predict the deterioration and shear failure of the foam core as core deterioration affects the integrity of the entire structure, influencing the stiffness of the structure and the resulting load-displacement curves.

To verify the accuracy of the numerically obtained  $G_{IIC}$  values, experimental tests such as the Cracked Sandwich Beam (CSB) test are necessary. Further investigations should be devoted to studying the effect on fracture toughness by the variation of the interleave veils thickness and aerial weight. In addition, this research can be expanded to other natural fibres that generally showcase weaker mechanical behaviour, such as jute, sisal etc., to be used as sources for nonwoven interleave veils.

## References

- [1] Kaufmann, J.: New Materials for Sports Equipment Made of Anisotropic Fiber-reinforced Plastics with Stiffness Related Coupling Effect. *Procedia Engineer*, 112 (2015), pp. 140–145. doi:10.1016/j.proeng.2015.07.189
- [2] Wang, W. (2004). Cohesive zone model for facesheet-core interface delamination in honeycomb FRP sandwich panels (Doctoral Thesis). West Virginia University.
- [3] Hamer, S.; Leibovich, H.; Green, A., Avrahami, R., Zussman, E., Siegmann, A., & Sherman, D.. Mode I and Mode II fracture energy of MWCNT reinforced nanofibrilmats interleaved carbon/epoxy laminates. *Composites Science and Technology*, 90 (2014), pp. 48–56. doi:10.1016/j.compscitech.2013.10.013
- [4] Gheryani, A. A.; Fleming, D. C.; Reichard, R. P.: Nonwoven polyester interleaving for toughness enhancement in composites. *Journal of Composite Materials*, 53(28-39) (2019), pp.4349-4367. doi:10.1177/0021998319857116
- [5] Kuwata, M.; Hogg, P. J.: Interlaminar toughness of interleaved CFRP using non-woven veils: Part 1. Mode-I testing. *Composites Part A: Applied Science and Manufacturing*, 42(10) (2011), 1551–1559. doi:10.1016/j.compositesa.2011.07.016
- [6] Bragagnolo, G.; Crocombe, A. D.; Ogin, S. L.; Mohagheghian, I.; Sordon, A.; Meeks, G.; Santoni, C.: Investigation of skin-core debonding in sandwich structures with foam cores. *Materials & Design*, 186 (2020). 108312. doi:10.1016/j.matdes.2019.108312
- [7] Gonzalez, A.; Mahfuz, H.; Sabet, M.: Enhancing Debond Fracture Toughness of Sandwich Composites for Marine Current Turbine Blades. *OCEANS 2019 MTS/IEEE SEATTLE*, (2019), pp. 1-7. doi:10.23919/oceans40490.2019.8962799
- [9] Quispitupa, A.; Berggreen, C.; Carlsson, L. A.. On the analysis of a mixed mode bending sandwich specimen for debond fracture characterization. *Engineering Fracture Mechanics*, 76(4) (2009), pp. 594–613. doi:10.1016/j.engfracmech.2008.12.008
- [9] Barbero, E. J.; Shahbazi, M.: Determination of material properties for ANSYS progressive damage analysis of laminated composites. *Composite Structures*, 176 (2017), pp. 768–779. doi:10.1016/j.compstruct.2017.05.074
- [10] Pierron, F.; Cerisier, F.; Grediac, M.: A Numerical and Experimental Study of Woven Composite Pin-Joints. *Journal of Composite Materials*, 34(12) (2000), pp. 1028–1054. doi:10.1177/002199830003401204
- [11] Spearing, S. M.; Evans, A. G.: The role of fiber bridging in the delamination resistance of fiber-reinforced composites. *Acta Metallurgica et Materialia*, 40(9) (1992), pp. 2191–2199. doi:10.1016/0956-7151(92)90137-4